ARCHIVES

of

FOUNDRY ENGINEERING

Mathematical Model of Bainitic Transformation in Austempered Ductile Iron

I. Olejarczyk-Wożeńska *, H. Adrian, B. Mrzygłód, M. Głowacki

AGH University of Science and Technology, Faculty of Metals Engineering and Industrial Computer Science
Department of Applied Computer Science and Modeling, ul. Czarnowiejska 66, 30-054 Krakow, Poland
* Corresponding author. E-mail address: iolejarc@agh.edu.pl

Abstract

A mathematical model of austenite - bainite transformation in austempered ductile cast iron has been presented. The model is based on a model developed by Bhadeshia [1, 2] for modelling the bainitic transformation in high-silicon steels with inhibited carbide precipitation. A computer program has been developed that calculates the incubation time, the transformation time at a preset temperature, the TTT diagram and carbon content in unreacted austenite as a function of temperature. Additionally, the program has been provided with a module calculating the free energy of austenite and ferrite as well as the maximum driving force of transformation. Model validation was based on the experimental research and literature data. Experimental studies included the determination of austenite grain size, plotting the TTT diagram and analysis of the effect of heat treatment parameters on the microstructure of ductile iron. The obtained results show a relatively good compatibility between the theoretical calculations and experimental studies. Using the developed program it was possible to examine the effect of austenite grain size on the rate of transformation.
.

Keywords: Modelling of phase transformations, Austenite - ferrite transformation, ADI, TTT diagrams

1. Introduction

Austempering within the range of bainitic transformation is one of the stages in the heat treatment of ductile iron to produce ADI. When the ductile iron is undercooled to a temperature below 550°C, the transformation of austenite into ferrite ($\gamma \rightarrow \alpha$) occurs. For many years there has been a fundamental controversy over the mechanism of austenite transformation in the bainitic range. Bainitic transformation is called intermediate transformation, as it exhibits the characteristics of both diffusion-induced and diffusionless phenomenon [3, 4].

On the one hand, bainitic transformation is treated as a transformation with the slip boundary formed by shear mechanism [3, 4], while bainite is treated as a lamellar product of the shear-induced phase transformation [5]. In the case of bainite growth caused by the effect of shear mechanism, various experimental studies are available to confirm that although the growth of bainite needles (stripes) is diffusionless, soon after this growth ends, the excess carbon from bainite is moved by diffusion to unreacted austenite [6]. As a consequence, the austenite is being gradually enriched in carbon until a point is reached at which its further transformation by the shear mechanism becomes thermodynamically impossible.

2. Model of austenite – ferrite transformation

2.1. Concept of the model

The examined model describing the kinetics of the growth of acicular ferrite in ADI utilizes the diffusionless bainite formation mechanism, taking into account the displacement of excess carbon from ferrite to unreacted austenite.

The model was based on a model developed by Bhadeshia [1] for modelling the bainitic transformation in high-silicon steels with inhibited carbide precipitation. The same model was later used by Ławrynowicz [7, 8] for modelling the ADI processing window. The original model includes:

- the effect of carbon displacement on the change in free energy under the assumption that with progress in transformation the driving force of the transformation $\Delta G_m, J/mole$ changes linearly between the initial (maximum) value $\Delta G_m^0, J/mole$ and the final value $G_N, J/mole$;
- autocatalytic effect – due to the increased density of nucleation sites with high ferrite volume fraction. It has been found that the autocatalysis factor β is a function of the mean carbon concentration in alloy, since an increase of the carbon content in austenite results in a decrease of the driving force due to the diffusion-induced transformation and thus inhibits autocatalysis [1, 8];
- influence of austenite grain size L,μm on the transformation rate;
- the phenomenon of incomplete transformation,
- changes in the volume fraction of bainitic ferrite needles as a function of the transformation temperature.

Taking into account the influence of the above factors, the time t, s, needed to achieve the required degree of transformation may be calculated from (1):

$$t = t_{ink} + t_{vv} \tag{1}$$

where:

$$t_{ink} = \frac{\exp\left(\frac{Q'}{R(T_{pi}+273)} + C_4\right)(T_{pi}+273)^z}{|\Delta G_m^0|^p} \tag{2}$$

$$t_{vv} = \frac{\exp(C)}{A(B+1)}\{\exp(E)(ln|1+B\xi| $$
$$+ f(-(E+D\xi)) - f(-E))$$
$$- \exp(-D)\left(\ln(1-\xi) + f(D(1-\xi)) - f(D)\right)\} \tag{3}$$

$$A = \frac{uK_1}{\theta} \tag{4}$$

$$B = \beta\theta \tag{5}$$

$$C = \frac{K_2}{RT_{pi}}\left(1 + \frac{\Delta G_m^0}{r}\right) \tag{6}$$

$$D = \frac{K_2(\Delta G_m^0 - G_N)}{rRT_{pi}} \tag{7}$$

$$E = \frac{D}{B} \tag{8}$$

$$f(x) = \frac{x}{1 \cdot 1!} + \frac{x^2}{2 \cdot 2!} + \cdots + \frac{x^n}{n \cdot n!} \tag{9}$$

$$G_N = 3.637(T_{pi} + 273) - 2540 \tag{10}$$

t_{ink}- incubation time, s,

t_{vv} – transformation time of normalized volume fraction of bainite, s,

Q', C_4, z, p - experimental constants: $Q' = 243200 \, J/mol$, $C_4 = -135, z = 20, p = 5$ [2],

T_{pi} - ausferritization temperature, ℃,

R - gas constant, $J/(mol \cdot K)$,

ΔG_m^0 - maximum free energy of nucleation, $J/mole$,

$u = u_t^2 u_w$ - unit volume of bainitic ferrite, μm^3,

u_t - length of ferrite needles, μm,

$u_w = 0.001077T - 0,2681$ - width of ferrite needles, μm^2

r - experimental constant: $r = 2540 \, J/mole$ [9],

$K_1 = (\bar{L}K_1')^{-1}$ - function of austenite grain size (the number of potential ferrite nucleation sites), $\frac{1}{mm^3 s}$,

$\bar{L}$ - mean grain size of austenite, μm,

K_1', K_2 - experimental constants: $\frac{K_1'}{u} = 0.57919E - 6 \, mm^2 s$, $K_2 = 0.20980E5 \, J/mole$, [1],

$\theta = \frac{x_{T_0'} - \bar{x}}{x_{T_0'} - x_\alpha}$ - maximum volume fraction of bainite,

$x_{T_0'}$ - carbon content at the T_0' boundary (Fig. 1), $mole$,

$\bar{x} = -1.7 + 0.0028 \cdot T_{aus} + 0.11Mn - 0.057Si - 0.058Ni - 0.12 \, Mo$ - average carbon content in alloy [10],

T_{aus} - austenitization temperature, ℃,

x_α - carbon content in ferrite, $mole$,

$\xi = v/\theta$ - relative volume fraction of bainite,

v - actual volume fraction of bainite,

$\beta = \lambda_1(1 - \lambda_2\bar{x})$ - autocatalysis factor,

λ_1, λ_2 - experimental constants: $\lambda_1 = 147.5, \lambda_2 = 30.327$, [1],

T_{pi} - ausferritization temperature, ℃,

G_N - universal nucleation function, $J/mole$,

In the examined model based on the shear mechanism it has been assumed that the inhibition of transformation occurs when carbon enriches austenite to the composition x_{T0} corresponding at the transformation temperature to the T_0 curve and the driving force of the shear-induced transformation decreases to zero (Fig. 1). The T_0 curve represents the location of all points in the temperature - carbon concentration graph where austenite and ferrite (stress-free) of the same chemical composition also have identical free energy. Owing to this, the austenite whose carbon concentration exceeds the value determined by the $T_0 (x_{T0})$ curve can not undergo the diffusionless transformation. The T_0 curve, modified to take into account the deformation energy in austenite due to the change of ferrite shape at the time of its growth, is called the T_0' curve [3, 8, 11].
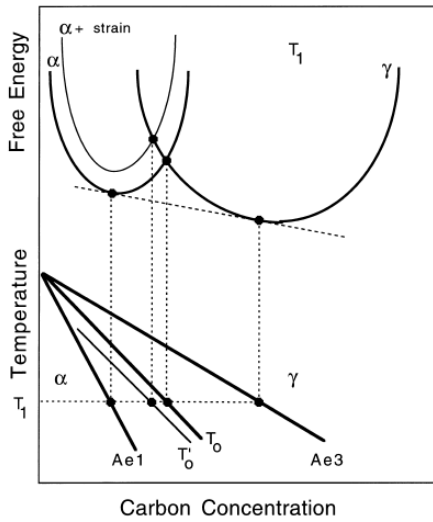
Fig. 1. Plotting the T_0 and T_0' curves [11]

2.2 Maximum free energy for nucleation

As mentioned previously, an assumption has been made in the model that with progress in transformation the driving force of the transformation ΔG_m, $J/mole$ changes linearly between the initial (maximum) value ΔG_m^0, $J/mole$ and the final value G_N, $J/mole$. As a universal nucleation function was adopted the function developed by Bhadeshia [1], calculated from formula (8). On the other hand, the maximum (initial) value of energy (ΔG_m^0) was determined from the thermodynamic models based on a CALPHAD method for the calculation of phase equilibrium systems [12, 13]. The CALPHAD method (CALculations of PHAseDiagrams) allows finding a relationship between the content of elements in a system and the equilibrium quantity of stable phases at a given temperature by using Gibbs free energy function G of phases occurring in the system. The basic thermodynamic properties of the φ phase used in the calculations are free energies of the pure components $^0G_i^\varphi$ and parameters of influence $L_{i,j}^\varphi$ of elements dissolved in the φ phase. The free energy functions G of the austenite and ferrite in an Fe-C system were described with a dual-lattice model of Hillert and Staffansson $(Fe, Mn, Si, Ni, V)_b(C, Va)_c$ with elements forming a substitution solution in one sublattice and carbon atoms and vacancies in another sublattice. For austenite $b = c = 1$, for ferrite $b = 1, c = 3$ [12].

The free energy of one mole of φ phase (where φ means austenite, γ, or ferrite, α) is represented by equation (11), respectively, [12, 14]:

$$
\begin{aligned}
G_m^\varphi = {} & y_{Fe}y_C \, {}^0G_{Fe:C}^\varphi + y_{Fe}y_{Va} \, {}^0G_{Fe:Va}^\varphi \\
& + y_{Mn}y_C \, {}^0G_{Mn:C}^\varphi + y_{Mn}y_{Va} \, {}^0G_{Mn:Va}^\varphi \\
& + y_{Si}y_C \, {}^0G_{Si:C}^\varphi + y_{Si}y_{Va} \, {}^0G_{Si:Va}^\varphi \\
& + y_{Ni}y_C \, {}^0G_{Ni:C}^\varphi + y_{Ni}y_{Va} \, {}^0G_{Ni:Va}^\varphi
\end{aligned}
\tag{11}
$$

$$
\begin{aligned}
& + y_V y_C \, {}^0G_{V:C}^\varphi + y_V y_{Va} \, {}^0G_{V:Va}^\varphi \\
& + bRT(y_{Fe}lny_{Fe} + y_{Mn}lny_{Mn} + y_{Si}lny_{Si} \\
& + y_{Ni}lny_{Ni} + y_V lny_V) \\
& + cRT(y_C lny_C + y_{Va}lny_{Va}) + {}^EG_m^\varphi \\
& + {}^{mg}G_m^\varphi
\end{aligned}
$$

where: $^EG_m^\varphi$ - the residual free energy of a given phase, $^{mg}G_m^\varphi$ - the contribution of magnetic effect to the free energy of the φ phase, $^0G_{i:Va}^\varphi$- Gibbs free energy of the i element of the φ phase, $^0G_{i:C}^\varphi$ - the free energy of the state in which all interstitial positions are filled with C atoms, y_i - the share of the positions of the i element (or Va vacancy) in one sublattice referred to the atomic fraction x_i of a given element in cast iron:

$$
y_C = \frac{x_C}{1 - x_C} \tag{12}
$$

$$
y_{Va} = 1 - y_C \tag{13}
$$

$$
y_{Fe} = \frac{x_{Mn}}{x_{Fe} + x_{Mn} + x_{Si} + x_{Ni} + x_V} \tag{14}
$$

$$
y_{Mn} = \frac{x_{Mn}}{x_{Fe} + x_{Mn} + x_{Si} + x_{Ni} + x_V} \tag{15}
$$

$$
y_{Si} = \frac{x_{Si}}{x_{Fe} + x_{Mn} + x_{Si} + x_{Ni} + x_V} \tag{16}
$$

$$
y_{Ni} = \frac{x_{Ni}}{x_{Fe} + x_{Mn} + x_{Si} + x_{Ni} + x_V} \tag{17}
$$

$$
y_V = \frac{x_V}{x_{Fe} + x_{Mn} + x_{Si} + x_{Ni} + x_V} \tag{18}
$$

The residual free energies of austenite $^EG_m^\gamma$ and ferrite $^EG_m^\alpha$ are represented by equation (19). L is the parameter of interaction between elements dissolved in the φ phase.

$$
\begin{aligned}
^EG_m^\varphi = {} & y_{Fe}y_{Mn}\left(y_C L_{Fe,Mn:C}^\varphi + y_{Va}L_{Fe,Mn:Va}^\varphi\right) \\
& + y_{Fe}y_{Si}\left(y_C L_{Fe,Si:C}^\varphi + y_{Va}L_{Fe,Si:Va}^\varphi\right) \\
& + y_{Fe}y_{Ni}\left(y_C L_{Fe,Ni:C}^\varphi + y_{Va}L_{Fe,Ni:Va}^\varphi\right) \\
& + y_{Fe}y_V\left(y_C L_{Fe,V:C}^\varphi + y_{Va}L_{Fe,V:Va}^\varphi\right) \\
& + y_C y_{Va}(y_{Fe}L_{Fe:C,Va}^\varphi + y_{Mn}L_{Mn:C,Va}^\varphi + y_{Si}L_{Si:C,Va}^\varphi \\
& + y_{Ni}L_{Ni:C,Va}^\varphi + y_V L_{V:C,Va}^\varphi)
\end{aligned}
\tag{19}
$$

The contribution of magnetic transformation to the Gibbs free energy of austenite and ferrite is described by formula (20) [12]:

$$
^{mg}G_m^\varphi = RTln(\beta + 1)f(\tau) \tag{20}
$$

$$
\tau = T/T_C \tag{21}
$$

for $\tau < 1$:

$$
f(\tau) =
$$
$$
1 - \left[\frac{79\tau^{-1}}{140p} + \frac{474}{497}\left(\frac{1}{p} - 1\right)\left(\frac{\tau^3}{6} + \frac{\tau^9}{135} + \frac{\tau^{15}}{600}\right)\right]/A \tag{22}
$$

for $\tau \geq 1$: $\tag{23}$

$$f(\tau) = \left(\frac{\tau^{-5}}{10} + \frac{\tau^{-15}}{315} + \frac{\tau^{25}}{1500}\right)/A$$

$$A = \frac{518}{1125} + \frac{11692}{15975}\left(\frac{1}{p} - 1\right) \tag{24}$$

where: T_C - Curie temperature, K, p - depends on the type of lattice and is equal to 0.28 for austenite and 0.4 for ferrite.

The described procedures for the calculation of free energy have been used in the thermodynamic analysis and to calculate the driving force component of austenite-ferrite transformation in the bainitic range. The maximum driving force of the transformation is related to a difference in the free energy of austenite (G_γ) and ferrite (G_α). Figure 2 shows the equilibrium conditions for both these phases at a temperature T_x. The state of equilibrium is defined by the minimum free energy. For the austenite of composition $\bar{x}$, in the state of equilibrium will remain the austenite with carbon concentration $x^{\gamma\alpha}$ and ferrite with carbon concentration $x^{\alpha\gamma}$. This corresponds to the values plotted by the tangent line which is common to both ferrite and austenite (Fig. 2a). The change in free energy accompanying the equilibrium transformation of one molar fraction of austenite is $\Delta G^{\gamma \to \alpha + \gamma'}$ (Fig. 2a). On the other hand, the free energy needed to form one molar fraction of ferrite (under conditions: austenite with carbon content $\bar{x}$ and temperature T_x) is denoted as ΔG_2. Since one molar fraction of the ferrite being formed is smaller than one molar fraction of the parent austenite, the change in free energy determined as ΔG_2 should be larger than the energy required for the formation of one molar fraction of austenite (Fig. 2a). It is determined by dividing $\Delta G^{\gamma \to \alpha + \gamma'}$ by $(x^{\gamma\alpha} - \bar{x})/(x^{\gamma\alpha} - x^{\alpha\gamma})$, which is the molar fraction of ferrite [3, 11, 2].
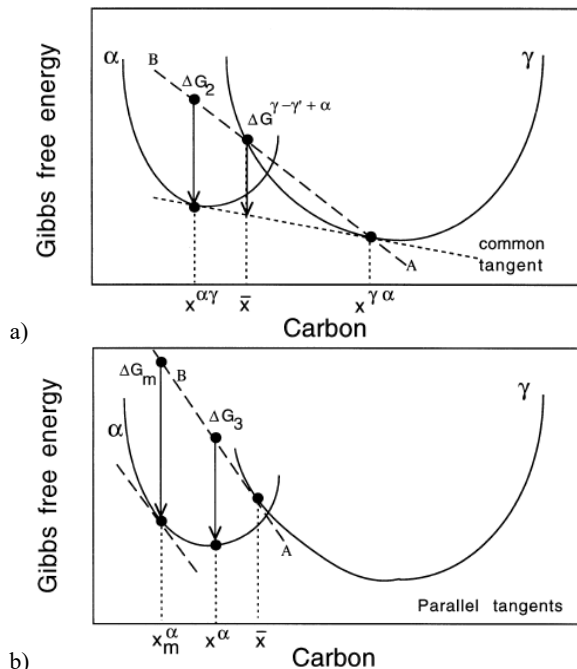
In the case of the examined transformation, the change in the composition of the austenite that remains unreacted is negligible and nucleation involves the formation of only a minimum amount of ferrite. The resulting amount of ferrite is so small that the composition of the residual austenite (parent phase) (x_γ) is almost identical to that of the primary austenite ($\bar{x}$). Then the change in free energy associated with the formation of one molar fraction of the ferrite nucleus can be determined in a manner similar to the determination of ΔG_2, taking, however, into account the fact that in the free energy graph, the tangent to the G_γ curve will pass through the point $\bar{x}$. Hence the change in free energy during the formation of one molar fraction of ferrite of the composition x_α will be given by ΔG_3 (Fig. 2b). In reality, a larger change in the free energy can be obtained by selecting the appropriate composition of the ferrite nucleus (x_m^α) using parallel tangent lines shown in Figure 2b. This maximum possible change in free energy will be denoted as ΔG_m.

All parameters used in calculations of the free energy of austenite and ferrite were taken from H. Adrian study [12].

2.3. The computer program

The described model has been implemented in the Visual Studio programming environment using C # language.

Input data to the program:
- temperature of isothermal transformation, T_{pi}, ℃,
- austenitization temperature, T_{aus}, ℃,
- percent degree of transformation, v, %,
- austenite grain size, $\bar{L}, \mu m$,
- chemical composition.

The developed program allows its user to calculate:
- time to obtain at a preset temperature the required degree of transformation – TTT diagram,
- free energy of austenite and ferrite and maximum free energy of nucleation,
- carbon content $x_{T_0'}$ in austenite as a function of the temperature of isothermal transformation.

The results of these calculations are presented in the form of graphs and saved to a file. Figure 3 shows examples of the calculation results.

a)

b)

Fig. 2. Changes in free energy during nucleation and growth of ferrite [3]
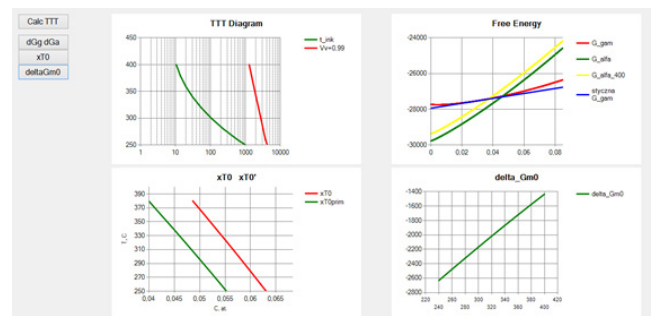
Fig. 3. Sample results of calculations a) the part of the TTT diagram, b) free energy of austenite and ferrite, c) carbon content in unreacted austenite (x_{T0} and x_{T0}'), d) the maximum driving force of transformation (ΔG_m^0)

3. Experimental

Experimental studies included the determination of austenite grain size, plotting the TTT diagram and analysis of the effect of heat treatment parameters on the microstructure of ductile iron with the chemical composition given in Table 1.

Table 1.
Chemical composition of the examined ductile iron.

Chemical composition, wt%						
C	Si	Mn	Mg	Ni	P	S
3.55	2.55	0.31	0.063	1.56	0.025	0.009

The austenite grain size was an input data to the developed model. To determine this size, a secant method was used. Samples of $\phi 20\ mm$ diameter and $20\ mm$ height were heated at $820, 870$ and $920\ ℃$ for 1 hour and then cooled in water. After heat treatment, the samples were ground and sections were prepared for etching. Etching was done with a reagent composed of 4 g picric acid, 100 ml H_2O and the addition of a surface tension reducing agent. This reagent reveals the boundaries of former austenite grains. As a next step, photographs of microstructures were taken at various magnifications using a Reichert optical microscope. Austenite grains were measured by the secant method using a SigmaScan Pro computer program calculating the mean of the measured secant lengths (300 to 500 measurements for each temperature). The results of the measurements are shown in Table 2. GS is a number of austenite grain size according of ASTM scale.

Table 2.
The size of austenite grains

T_{aus}, ℃	820	870	920
$\bar{L}, \mu m$	105	107	98
GS	3	3	3

Dilatometric studies and TTT diagram developed for the examined cast iron were discussed in [15]. Based on this diagram, 18 heat treatment variants have been planned. A detailed description of these studies and an analysis of the effect of heat treatment parameters on the microstructure and progress in austenite - ferrite transformation are presented in [16, 15].

4. Results and discussion

Using the developed program, a TTT diagram was plotted for the temperature range of $240 - 400\ ℃$, chemical composition given in Table 1 and austenitization temperature of $T_{aus} = 920\ ℃$. The obtained results were compared with an experimental TTT diagram [15], as shown in Figure 4.

The results of calculations presented in the paper were obtained for a constant austenitization temperature, since the experimental studies presented in [15, 16], which served as a basis for the verification, used only one austenitization temperature. In the model it is possible to change this parameter in the range of

$820 \div 950\ ℃$, but it does not really affect the TTT graph obtained by calculations.
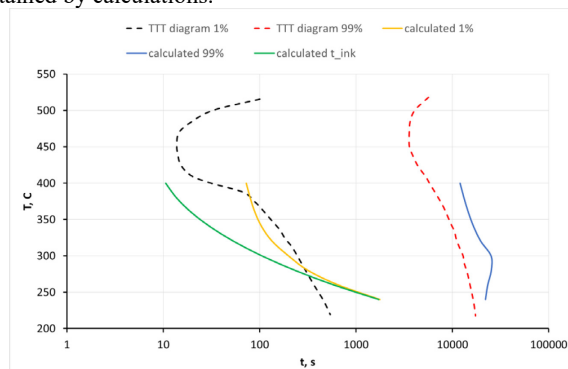
Fig. 4. TTT diagram: dashed line - experimental curve, solid line - calculated curve

From the analysis of the results obtained it follows that a relatively good compatibility has been obtained for the starting stage of transformation. The differences can be attributed to, among others, small number of points available when plotting the TTT diagram.

On the other hand, significant differences are visible at the end of the transformation. As the experimental studies show, the austenite-ferrite transformation ends much earlier than it results from the calculations made by the developed computer program. Studies have revealed the necessity to refine the constants used in the presented model for example by inverse analysis or to re-plot the TTT diagram.

Verification of calculations of the maximum driving force of transformation (ΔG_m^0) and carbon content in unreacted austenite (x_{T0}, x'_{T0}) was based on the calculations presented by Ławrynowicz [8], as shown in Figures 5 and 6.
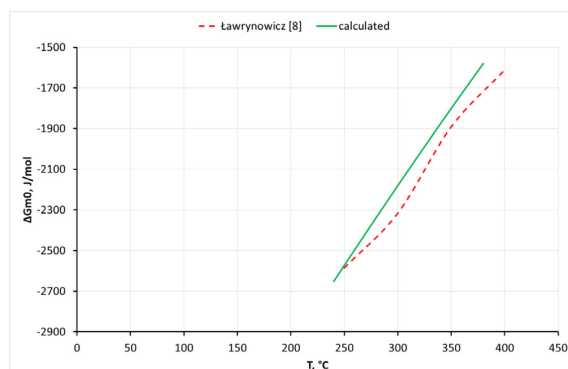
Fig. 5. The maximum driving force of transformation, dashed line – the results of calculations made by Ławrynowicz [8], solid line - the results of calculations made by the developed model
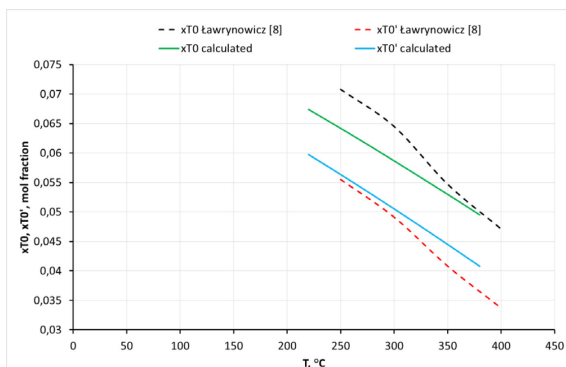
Fig. 6. Carbon content in unreacted austenite: dashed line - the results of calculations made by Ławrynowicz [8], solid line - the results of calculations made by the developed model

Careful analysis of the results shown in Figure 5 regarding the maximum driving force of transformation leads to the conclusion that calculations made by the developed program are correct. On the other hand, the calculated values of the carbon content in unreacted austenite (Fig. 6) show slight differences when compared with the results presented by Ławrynowicz [8], which may be due to differences in the thermodynamic data used to calculate the free energy of the phases present.

Using the developed program, the effect of grain size on the transformation rate was examined, as shown in Figure 7.
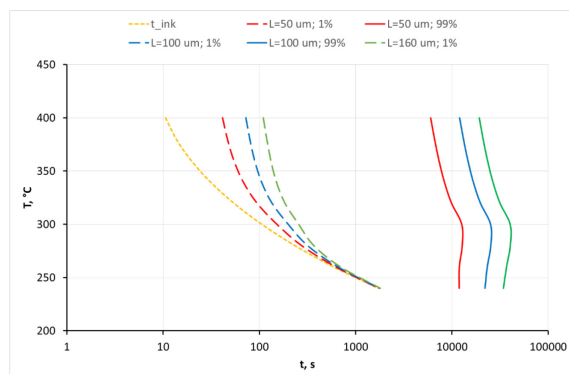
Fig. 7 Austenite grain size vs austenite-ferrite transformation rate

As shown in Figure 7, the austenite grain size has a significant effect on the transformation rate.

5. Summary

Computers technologies are an important tool aiding the optimization process of the Fe-C alloys microstructure and properties. There are currently available as a cheap and effective way of optimization, are used for modelling and analysis of phenomena occurring in many areas of research [17-19]. Computer simulations allow reproducing with the use of mathematical models the course of industrial processes and analysis of properties of the tested materials.

A mathematical model has been developed, implemented and validated to study the austenite - ferrite transformation kinetics. For a given chemical composition, the developed program allows calculating the following parameters:
- TTT diagram for a preset temperature range,
- free energy of austenite and ferrite,
- maximum driving force of transformation,
- carbon content in unreacted austenite,

It is also possible to examine the effect of austenite grain size on the transformation rate.

The conducted analysis has revealed the need to complete and repeat some of the experimental studies. It is planned to perform further research and modify and extend the model to provide it with an option to calculate the volume fraction of ferrite.

Acknowledgements

References

[1] Chester, N.A. & Bhadeshia, H. (1997). Mathematical modelling of bainite transformation kinetics. *Journal de Physique IV.* C5(7), 41-46.
[2] Bhadeshia, H. (1982). Thermodynamic analysis of isothermal transformation diagrams. *Metal Science.* 16, 159-165.
[3] Bhadeshia, H. (2001). *Bainite in steels. Transformations, microstructure and properties.* 2 red., Cambridge: Institute of Materials.
[4] Ławrynowicz, Z. & Dymski, S. (2006). Mechanism of bainitic transformation in ADI. *Archives of Foundry.* 6(19), 171-176. (in Polish).
[5] Bhadeshia, H. & Edmonds, D.V. (1980). The mechanism of bainite formation in steels. *Acta Metallurgica.* 28(9), 1265-1273.
[6] Bhadeshia, H. (1981). A rationalisation of shear transformations in steels. *Acta Metallurgica.* 29(6), 1117-1130.
[7] Ławrynowicz Z. & Dymski, S. (2006). Application of bainitic transformation mechanism for ADI cast iron window molding. *Archiwum Odlewnictwa.* 6(19), 177-182. (in Polish).
[8] Ławrynowicz, Z. (2016). Kinetics of the bainite transformation in austempered ductile iron ADI. *Advances in Materials Science.* 16(2), 47-56.
[9] Rees, G.I. & Bhadeshia, H.K. (1992). Bainite transformation kinetics. Part1 Modified model. *Materials Science and Technology.* 8, 985-993.
[10] Chang, L.C. (2003). An analysis of retained austenite in austempered ductile iron. *Metallurgical and Materials Transactions A.* 34A, 211-217.
[11] Ławrynowicz, Z. (2009). *Attempt to use the bainitic transformation mechanism to model kinetics and microstructure of low alloy steel.* Bydgoszcz: Wydawnictwa

Uczelniane Uniwerystetu Technologiczo-Przyrodniczego. (in Polish).

[12] Adrian, H. (2011). *Numerical modeling of heat treatment processes.* Kraków: Wydawnictwa AGH. (in Polish).

[13] Wróbel, M. & Burbelko, A. (2014). CALPHAD method - modern technique for obtaining thermodynamic data. *Archives of Foundry Engineering.* 14(spec.3), 79-84. (in Polish).

[14] Huang, W. (1991). Termodynamic properties of the Fe-Mn-V-C system. *Metallurgical Transactions A.* 22A, 1911-1920.

[15] Mrzygłód, B., Kowalski, A., Giętka, T. & Głowacki, M. Characteristics of ADI ductile cast iron with single addition of 1.56% Ni. *Archives of Metallurgy and Materials,* at editor

[16] Olejarczyk-Wożeńska, I., Mrzygłód, B., Giętka, T., Kowalski, A. & Adrian, H. (2017). Effect of austempering parameters on microstructure of ADI with 1.5% Ni. METAL 2017: 26th International Conference on Metallurgy and Materials. Ostrava: TANGER.

[17] Kluska-Nawarecka. S., Gorny, Z. & Wilk-Kolodziejczyk, D. et al., (2007). The logic of plausible reasoning in the diagnosis of castings defects. *Archives of Metallurgy and Materials.* 52(3), 375-380.

[18] Nawarecki, E., Kluska-Nawarecka, S. & Regulski, K. (2012). Multi-aspect character of the man-computer relationship in a diagnostic-advisory system, Human – computer systems interaction: backgrounds and applications 2, eds. Zdzisław S. Hippe, Juliusz L. Kulikowski, Teresa Mroczek. — Berlin; Heidelberg: Springer-Verlag.

[19] Kluska-Nawarecka, S. Regulski, R., Krzyżak, M., Leśniak, G. & Gurda, M. (2013). System of semantic integration of non-structuralized documents in natural language in the domain of metallurgy. *Archives of Metallurgy and Materials.* 58(3), 927-930.